SLAC-PUB-10390

New Formulation of the Synthesis Problem in Electron Optics

V. Ivanov
Stanford Linear Accelerator Center

V. Brezhnev
Eon-Bo Ltd., Novosibirsk, Russia

Submitted to Nuclear Instrumentation and Methods (NIM) A

Stanford Linear Accelerator Center, Stanford University, Stanford, CA 94309

Work supported by Department of Energy contract DE–AC03–76SF00515.

New formulation of the synthesis problem in electron optics

V. Ivanov*
Stanford Linear Accelerator Center, USA
V. Brezhnev
Eon-Bo Ltd., Novosibirsk, Russia

May 30, 2003

Abstract

We describe a new approach to solving the problem of harmonic field synthesis for electron-optical systems. Numerical solutions obtained in practice with the classical approach often lead to operational difficulties, such as numerical instability and vacuum breakdown. Our approach differs from the classical one in that it considers a mixed formulation where one part of the information is responsible for representing objective functionals - Cauchy data, while the other part of the information represents the boundary conditions defined on boundaries of specified geometry. This approach takes into account the a priori structural constraints of the synthesis problem, analytically extending the solution to the subdomain of synthesis as well as finding the tolerances for small perturbations of the objective functional. Numerical algorithms proposed in this work are based on the integral representation of a field by a potential of a single and double layer as well as by a volume potential for charged particle beams. A classification of the basic types of electronic lenses with minimal abberations is given. Numerical examples of test and practical problems are presented. This approach is implemented in the code "Synthesis-2" of Computer Aided Design system "TOPAZ".

PACS: 41.20.Cv; 02.70.Pt; 42.30.Va
Keywords: Electromagnetism; Boundary element method; Electron optics

1 Introduction

We will consider the synthesis of electromagnetic fields with prescribed properties. It is common to split the process of this design for various kind of devices into the problems of analysis, optimization and synthesis. A simple example of electron-optical system (EOS) design is the analysis of an electro-magnetic field distribution and the trajectories of charged particles for given geometry, fixed potentials of the electrodes, excitation currents of magnetic lenses and parameters of dielectric and magnetic materials. It seems to be a more complex problem to optimize the EOS parameters when there is a need to provide optimal quality-criteria for an optical system by varying the geometry parameters, electrode potentials and excitation currents. But in this case the device's structure has already been defined, and fundamentally new solutions are not expected. Besides, when common assumptions are made concerning the problem's functionals there are other questions to be answered: choosing an initial approximation which insures existence and uniqueness of the solution; this approximation discovers a successful solution in the case of non-linear objective functionals and technical limitations of the problem.

*Correspondence address: 2575 Sand Hill Rd., Menlo Park, CA, 94025, USA. E-mail: ivanov@slac.stanford.edu

The most complete answer to the problems of device design requires solving a synthesis problem in which the structure of the optical system is not yet defined, but is determined by functionals which characterize the device's optical parameters. We would point out that prior to the computer era and the introduction of sophisticated numerical methods, design of an EOS was usually defined in terms of a synthesis problem. The major achievements in this direction were obtained by J. Pierce [1], B. Meltzer [2], P. Lomax [3], P. Kirshtein [4, 5], K. Harker [6], W. Tretner [7], M. Szilagyi [8], V. Ovcharov [9]-[14], V. Danilov [15]-[17], V. Syrovoy [18]-[20], Shanturin [21] *etc.* The generally accepted formulation of an EOS synthesis problem consists of an internal and external problems. In the first of them there is a need to determine the characteristics of the motion of a charged particle beam with specified phase volume, as well as space current distribution. The external problem should determine a field distribution outside the beam to determine the configuration of electrodes, magnetic circuits and solenoids, which ultimately forms a beam with the given parameters. When solving the internal problem an engineer defines a set of functionals $F_i, i = 0, \ldots, m$, which depends on distribution of electric and magnetic fields in the region through which the beam passes. One of these functionals F_0 is the objective functional, and the others correspond to technical constraints. Examples of these functionals are the beam envelope, the energy characteristics of a beam and criteria of the image quality: magnification, cross-over and Gauss' plane positions, the values of aberrations, spatial and temporal resolutions of a device. The goal of this internal synthesis problem is to determine the configuration of the fields along the axis or along the beam's boundary which corresponds to the given values of functionals F_i. In numerical solution we define a set of N points along some line S_0 and a complete system of functions $\psi_j, j = 1, \ldots, N$, which extends the finite-dimension field representation $\psi(s) = \sum_j \alpha_j \psi_j(\tau)$. Here τ is a parametric coordinate for this line, which can be a portion of the axis or of the beam boundary. A set of polynomial functions ψ_j is often used. The minimization of the objective functional F_0 is achieved by varying the polynomial coefficients α_i, using well-known optimal control methods [22].

The external problem of synthesis is split into several stages. First, the field should be extrapolated from the axis or the beam boundaries into the whole space, then the set of equipotential lines is built, and technologically easy-to-manufacture shapes are chosen for the electrodes, solenoids and magnetic circuits such that they approximate the synthesized field with a given accuracy. The solution error is inferred by replacing the synthesized surfaces with the simplified ones, taking into account aperture holes not envisioned in the prior problem formulation, and truncating the electrodes to limit the dimensions of device. All these factors contribute to a more or less substantial deviation for the electron-optical functional values given originally from the values computed using direct calculation for the system obtained in synthesis. That is why, during the final design stage, there is a need to optimize the synthesized system. The important difference between this final stage and solving the ordinary optimization problem (without known good initial approximation) is the initial approximation which, in this case, is the synthesized solution. This guarantees the existence of a solution in the vicinity of the initial approximation and fast convergence of the optimization problem. Additional benefit of our approach is that the manufacturing tolerances can be determined simultaneously during the final solution stage.

The most complicated and laborious stage of the EOS synthesis problem is the extrapolation of harmonic fields from some prescribed line S_0 into the whole space. If, in a particular case, S_0 is the axis of a cylindrical system, the solution is given by the Scherzer series for the scalar potential ϕ in cylindrical coordinates r, z:

$$\phi(r, z) = \sum_{i=0}^{\infty} \frac{(-1)^i}{(i!)^2} \left(\frac{r}{2}\right)^{2i} \Phi^{(2i)}(z),\ \Phi(z) \equiv \phi(0, z). \tag{1}$$

In the general case it is possible to write down the appropriate multipole expansion for the

potential. The most complex part of the practical usage of the Scherzer series is calculation of the higher derivatives of the axial field $\Phi^{(i)}(z)$ – the Cauchy data, which are known with a certain precision. Let the initial data be defined on a line segment of length L. As shown in [23], the 1% error in the field extrapolation is observed on the distance $r/L < 0.15$, where L is the length of a section with the initial data. In some publications [24]-[25] the solution of the above mentioned problem has been achieved using the finite-difference approximation of Cauchy problem for the Laplace equation and fitting algorithms for smoothing a finite-difference solution or reducing it to the Cauchy problem for the system of ordinary differential equations for the line method. For these methods it is possible to increase the stability interval up to $r/L < 0.4$ for sufficiently smooth initial data. The method of conformal mapping has similar problems of numerical precision [27]-[29]. Here the authors obtain 10% of error in the potential evaluation on the distance $r/L = 0.4$ from the beam boundary.

Most researchers have made substantial efforts to overcome the purely mathematical difficulties associated with the necessity of solving conditionally-correct problems and building the different algorithms of regularization. From our point of view most of such mathematical formalizms do not reflect practical limitations. Let us explain this with examples. The classical example of solving the synthesis problem is the Pierce gun model. The solution of the internal problem for this gun, which produces a cylindrical beam, is given by the Child-Langmuire law for emission current density j:

$$j(z) = \frac{4}{3}\varepsilon_0\sqrt{\frac{2|q|}{m}}\frac{\Phi^{3/2}(z)}{z^2}, \quad \Phi(z) = Cz^{4/3}, \tag{2}$$

but for the external problem the field distribution has the following form

$$\phi(r,z) = C(r^2+z^2)^{2/3}\cos\left(\arctan\frac{r}{z}\right). \tag{3}$$

Here q is the particle charge, m is its mass, and ε_0 is the permittivity of free space. The constant C can be determined from the condition $\Phi(d) = U$, where d is a diode gap and U is an accelerating potential. It is clear that the exact implementation of this model gives two electrodes of a certain shape and of infinite extent. In practice such a system could be reproduced only approximately since the electrode size must be finite. This is accomplished by designing the electrode-support mechanism and by deforming the electrodes appropriately to compensate for the field perturbations caused by finite electrode size. Additionally, it is necessary to provide an aperture hole in the anode, to enable the beam to pass through. When the Pierce diode's length is much less then its radius, the anode hole has the effect of a strong defocusing lens. This effect could be reduced by introducing an intermediate correcting electrode or by deforming the anode surface. The book by Molokovsky and Sushkov [26] contains real gun design examples. The comparison of two pictures in Fig.1 shows that the model of the ideal Pierce gun and the practical device from [26] are so different that the only way to make a realistic design is, first, to solve the synthesis problem, and then modify this solution in order to take into account additional technical requirements by solving an optimization problem.

The numerous examples of solving the synthesis problem in its classical formulation show that the results are far from their practical realization. One of these results from [28] is given in the Fig. 2. It shows clearly that the solution include areas of the high gradient field which are unsafe for vacuum breakdown.

The solution of the synthesis problem can be visualized by a set of equipotential lines. Some of these lines can represent the surfaces of conducting electrodes. It is easy to show that in classical formulation all of these surfaces must cross the axis, so it is impossible to synthesize the electrode

with a hole on axis by using classical formulation of the synthesis problem. The maximum principle for harmonic functions shows that the solution of the Cauchy problem for the Laplace equation can not give a closed or limited contour of equipotential line which is not connected with the boundary. The existence of such a contour is only possible when the field sources are placed inside the contour. We obtain these contours by introducing the surfaces with the field sources into the solution domain. We will call these surfaces "skeleton" source surfaces. Further these contours will be used to form the electrodes.

The real goal of our argument is to show that the complexity of solving the synthesis problem for practical devices is not concerned with overcoming the mathematical difficulties of solving ill-conditioned problems of harmonic field extrapolation. This problem can be resolved in terms of the new formulation which reflects the practical requirements of device design. The main ideas of this approach have been published by the authors in [30],[34]. We call this the "practical" approach.

2 Integral representations in synthesis problems

The necessity to take into account given technical requirements leads us to the mixed formulation of the synthesis problem with two types of initial data. The first type is Cauchy data on the axis, which is responsible for reproducing the field quality in the paraxial subdomain of the problem. The second type are boundary values on fixed-shape surfaces that satisfy additional technical requirements.

Following our new formulation of the synthesis problem, the complete algorithm consists of the following steps:

1. Obtain the Cauchy data by minimizing the quality functional F_0 of the EOS;
2. Introduce three types of surfaces determined by the initial data for the EOS:
   a) the "normal" surface with specified boundary conditions and geometry, which describes the given elements of the construction - electrodes and dielectrics;
   b) the "skeleton" surface with specified geometry but with unknown field source distribution (as charges σ and dipoles ν), which is the basis of synthesized electrodes;
   c) "Cauchy" surface with given Cauchy data obtained at step 1 or with continuity conditions on the "free" boundaries of an embedded fragment to make the analytical continuation through these boundaries.
3. Obtain the field source distribution on the surfaces a) and b), taking into account the space charge of the beam. This distribution should minimize the residual of the numerical solution for the given conditions on the surfaces a) and c) in addition to limiting the potential discontinuity across surfaces c);
4. Draw a set of equipotential lines of the calculated field. Obtain the "band of tolerance" - the area of displacement for these lines caused by varying the problem limitations F_j;
5. Put in the "engineered" shapes of the electrodes in the "band of tolerance". This step can not be formalized automatically. It can be done only "by hand";
6. Solve the direct problem of electron optics with the obtained electrodes to verify the quality of the optics.

Now we will give the general mathematical formulation of the synthesis problem. It can be done in the following way. There is a multi-connected piece-wise smooth boundary S with boundary conditions $\psi(s)$

$$\left(\alpha\phi + \beta\frac{\partial\phi}{\partial\vec{n}}\right)_S = \psi(s), \tag{4}$$

and a smooth surface (or line) S_0 with given Cauchy data $\Phi(\tau)$ in parametric form

$$\phi|_{S_0} = \Phi(\tau), \tag{5}$$

where α, β are given constants,s and τ are arguments for parametric representations of both surfaces and $\vec{n}$ is a unit vector of the outer normal on the boundary.

By introducing an additional ("skeleton") surface Γ with field sources of charge density σ and dipole density ν we can obtain a system of integral equations for these sources

$$\begin{aligned}
\psi(s) &= \int_{\Gamma^*} \sigma(t)\left[\alpha + \beta\frac{\partial}{\partial\vec{n}}\right] G_\sigma(s,t)d\Gamma + 2\pi\beta\sigma(s) + \\
&\quad \int_\Gamma \nu(t)\left[\alpha + \beta\frac{\partial}{\partial\vec{n}}\right] G_\nu(s,t)d\Gamma + 2\pi\alpha\nu(s), \quad s \in S,\, t \in \Gamma^*, \Gamma^* = \Gamma \cup S, \qquad (6)\\
\Phi(\tau) &= \int_{\Gamma^*} \sigma(t)G_\sigma(\tau,t)d\Gamma + \int_\Gamma \nu(t)g_\nu(\tau,t)d\Gamma + 2\pi\nu(\tau), \quad t \in \Gamma^*,\, \tau \in S_0. \qquad (7)
\end{aligned}$$

This system can be rewritten in the operator form

$$\hat{G}\mathbf{X} = \mathbf{F}, \tag{8}$$

where $\mathbf{X} = \left\{ \begin{array}{c} \sigma \\ \nu \end{array} \right\}$ is a source vector, and $\mathbf{F} = \left\{ \begin{array}{c} \psi \\ \Phi \end{array} \right\}$ is a right-hand vector of initial data, $\hat{G}$ is an integral operator of the system.

The Green functions which correspond to the kernels of single-layer and double-layer potentials in 3D are given by the formulas

$$G_\sigma(P,Q) = \frac{1}{4\pi\varepsilon_0 R_{PQ}}, \quad G_\nu(P,Q) = \frac{\partial}{\partial\vec{n}_Q}\left(\frac{1}{4\pi\varepsilon_0 R_{PQ}}\right). \tag{9}$$

Here R_{PQ} is the distance between an observation point $P(s)$ and a source point $Q(t)$, ε_0 is the permittivity of a free space.

3 Numerical solution algorithm

The complete set of equations for high-current stationary electron optics includes the field equations (described above), the equation of motion for a relativistic particle with mass m and charge q in the Lorentz form

$$\dot{\vec{p}} = q(\vec{E} + [\vec{v} \times \vec{B}]), \quad \vec{p} = \frac{m\vec{v}}{\sqrt{1 - (\vec{v}\vec{v})/c^2}}, \tag{10}$$

and conservation law for the total current

$$\mathrm{div}\vec{j} = 0, \quad \vec{j} = \rho\vec{v}, \tag{11}$$

where $\vec{E} = -\nabla\phi$ is the electric field strength, $\vec{B}$ is the magnetic field induction, $\vec{p}$ is the momentum of a particle, $\vec{v}$ is its velocity, c is the speed of light in free space, $\vec{j}$ is the beam current density.

We must also define initial conditions for the emitted/injected beam. For space charge limitations they can be defined by setting the normal component of self-consistent electric field E_n to zero on the emitter surface $(E_n)_S = 0$. The total self-consistent electric field at observation point $\vec{r}$ is defined by superposition external and beam fields

$$\vec{E}(\vec{r}) \equiv -\nabla(\phi + \phi_\rho) = -\nabla\phi - \frac{1}{4\pi\varepsilon_0}\int_V \rho(\vec{r}')\nabla\frac{1}{|\vec{r}-\vec{r}'|^3}d^3\vec{r}', \tag{12}$$

where ϕ is the potential of the external sources (electrodes), and ϕ_ρ is the potential of space charge of the beam. The magnetic induction is defined in a similar way

$$\vec{B}(\vec{r}) = \vec{B}_0(\vec{r}) + 4\pi\mu_0\int_V \frac{\vec{j}(\vec{r}')\times(\vec{r}-\vec{r}')}{|\vec{r}-\vec{r}'|^3}d^3\vec{r}', \tag{13}$$

where μ_0 is the permeability of free space, $\vec{B}_0$ is the induction of external sources (coils or iron magnets), and the volume integral corresponds to the self-consistent magnetic field of the relativistic beam.

The numerical model and algorithms of self-consistent fields are accurately described in [32]. This is the quasi-laminar model, which can take into account the motion of non laminar flows for different kinds of charged particles, as well as energy and angular distribution for emitted particles.

In numerical approximation of the system of integral equations (8) we use the method of interpolation and boundary collocation, described in [32]. Here the boundary surfaces S and Γ are represented by parametric equations for piece-wise smooth segments

$$x = x_i(\tau), \quad y = y_i(\tau), \quad \bar{\alpha}_i \le \tau \le \bar{\beta}_i, \quad i = 1, \ldots, \bar{M} \tag{14}$$

with given constants $\bar{\alpha}_i$ and $\bar{\beta}_i$. Some set of n_i points $\tau_{ij}, j = 1, \ldots, n_i$ is defined for each of the $\bar{M}$ segments.

The solution $X(t)$ of system (8) is approximated by cubic splines

$$\mathbf{X}(t) = M_{j-1}\frac{(t_j-t)^3}{6h_j} + M_j\frac{(t-t_{j-1})^3}{6h_j} + \left(\mathbf{X}_{j-1} - M_{j-1}\frac{h_j^2}{6}\right)\frac{t_j-t}{h_j} + \left(\mathbf{X}_j - M_j\frac{h_j^2}{6}\right)\frac{t-t_{j-1}}{h_j}, \tag{15}$$

where $\mathbf{X}_j \equiv \mathbf{X}(s_j)$, $h_j = t_j - t_{j-1}$, $j = 1, ..., n_i$. The coefficients M_j of the spline function can be evaluated from the continuity condition for the second derivative of the solution $\mathbf{X}$ at the internal points of approximation on the boundary curves [35]. According to this book, we substitute the spline representation (15) into the the integral equations (8), and satisfy the boundary conditions at the set of collocation points on the boundary contour. In our case the sets of the approximation and the collocation points t_j are not identical. Let the total number of points on the surface S be equal to N_1, on Γ - N_2, on S_0 - N_3. Then total number K of collocation points equals $N_1 + N_3$, but total number of source points N equals $N_1 + 2N_2$. We multiply N_2 by 2 because the surface Γ has double set of sources σ and ν. As a result of this procedure we obtain a rectangular matrix $\hat{A}$ of dimension $N \times K$ for the linear system $\hat{A}\mathbf{X} = \mathbf{F}$, which corresponds to the operator equation 8. The stability of the numerical solution for this linear system can be increased if the original problem is formulated in the weak or variational form, that is, by minimizing the functional

$$\mathcal{F} = (\mathbf{X}^*\hat{G}^* - \mathbf{F}*)(\hat{G}\mathbf{X} - \mathbf{F}), \tag{16}$$

which corresponds to the Euler equation $\hat{G}^*\hat{G}\mathbf{X} = \hat{G}^*\mathbf{X}$, where symbol '*' denotes a conjugate operator or vector.

The enlargement of a class of possible solutions is realized by introducing the modified functional

$$\mathcal{F}_{\mathcal{D}} = (\mathbf{X}^*\hat{G}^* - \mathbf{F}^*)\hat{D}(\hat{G}\mathbf{X} - \mathbf{F}), \tag{17}$$

where $\hat{D}$ is diagonal operator with weight ratios w_i, which correspond to separate fragments of the surface Γ. These ratios reflect the influence of separate electrodes or "skeleton" surfaces on the quality of synthesized solution. By varying these ratios one can determine the tolerance band for variation of electrode shapes corresponding to acceptable deviation of electron optical parameters.

The final linear system can be obtained by symmetrization of the matrix A with diagonal matrix D as

$$\hat{C}\mathbf{X} = \hat{A}^t\mathbf{F}, \quad \hat{C} \equiv \hat{A}^t D\hat{A}, \tag{18}$$

where weight ratios w_i have been added to the diagonal elements of symmetric matrix $\hat{C}.A^t$ is transpose of A.

We use the Gauss quadrature formulas for evaluation of the integrals over the boundary, and a modified Gaussian elimination procedure to solve the linear system.

The Green functions in 2D Cartesian coordinates are given by the formulas

$$G_\sigma(x,y;x',y') = \frac{1}{2\pi\varepsilon_0}\ln[(x-x')^2 + (y-y')^2], \tag{19}$$

$$G_\nu(x,y;x',y') = \frac{1}{\pi\varepsilon_0}\frac{(x-x')\cos(\vec{n}\vec{e}_x) + (y-y')\cos(\vec{n}\vec{e}_y)}{(x-x')^2 + (y-y')^2}. \tag{20}$$

In the axially symmetric case these formulas are

$$G_\sigma(r,z;r',z') = \frac{r'K(k)}{\pi\varepsilon_0\delta}, \quad \delta = \sqrt{(r+r')^2 + (z-z')^2}, \tag{21}$$

$$G_\nu(r,z;r',z') = \frac{1}{\pi\varepsilon_0\delta}\left\{\frac{r'}{2r}\left[\frac{(r')^2 - r^2 + (z-z')^2}{\delta}E(k) - K(k)\right]\cos(\vec{n}\vec{e}_r) + \frac{r'(z-z')E(k)}{(r-r')^2 + (z-z')^2}\cos(\vec{n}\vec{e}_z)\right\}, \tag{22}$$

where $K(k)$ and $E(k)$ are complete elliptic integrals of the first and second kind which depend on the parameter $k^2 = 4rr'/\delta$, $\vec{e}_x, \vec{e}_y$ and $\vec{e}_r, \vec{e}_z$ are the unit vectors of the coordinate systems.

We developed the analytical technique to normalize kernel and edge singularities in order to obtain high precision of calculations as is described in [32].

4 Basic set of lenses forming cylindrical beams

One of the most common problem in electron optics is the problem of generating cylindrical beams of charged particles. Let us consider one of text book examples of electron optic problems. We will show that the classical formulation of the synthesis problem is not able to give a practical solution. In forming cylindrical beams the main requirement on the field is that the radial component should be proportional to radius $E_r \sim r$. The simplest example for this field is the well known Butler lens. Its on-axis potential is represented by a cubic parabola

$$\Phi(z) = 3\Phi_0\left(\frac{z}{L}\right)^2\left(1 - \frac{2z}{3L}\right), \quad 0 \le z \le L, \tag{23}$$

where L is the lens length and Φ_0 is the accelerating potential.

By adding the symmetric continuation

$$\Phi_+(z) = \Phi_0 \left\{ 1 - \left(\frac{z}{L}\right)^2 \left[1 - \frac{2}{3}\left(\frac{z}{L} - 1\right)\right]\right\}, \quad L \le z \le 2L, \tag{24}$$

we obtain a set of two lenses - focusing and defocusing. The continuity conditions in this case must set $\Phi(L) = \Phi_+(L), \Phi'(L) = \Phi'_+(L), \Phi''(L) = \Phi''_+(L)$. The off-axis potential distribution for this composite lens is

$$\phi_+(r,z) = \begin{cases} \Phi_0 \left[3\left(\frac{z}{L}\right)^2 \left(1 - \frac{2z}{3L}\right) - 3r^2 \left(\frac{1}{2} - \frac{z}{L}\right)\right], & 0 \le z \le L, \\ \Phi_0 \left[1 - 3\left(\frac{z}{L} - 1\right)^2 \left(1 - \frac{2}{3}\left(\frac{z}{L} - 1\right)\right) - 3r^2 \left(\frac{3}{2} - \frac{z}{L}\right)\right], & L \le z \le 2L. \end{cases} \tag{25}$$

Figures 3 and 4 represent on-axis and potential distributions for that composition in two cases: symmetrical – ϕ_+ and antisymmetrical – ϕ_- discussed below. It is clear that no contrivances can obtain the shape of the electrode dividing both lenses in solving the Cauchy problem with a classical formulation, i.e. to obtain the branching point on the axis and equipotential domain inside the boundary of the central electrode. The only possibility is to get such contour by placing the field sources of unknown density σ inside them. The values of σ can be determined by satisfying to the Cauchy data on the axis.

A remarkable thing in this problem is that the regions of both lenses really isolated one from another, and perturbation of the field in one of them can not affect to the field in an other domain. But smooth axial potential distribution "does not know" about that because it is not possible to draw a conclusion about this isolation by looking at the axial distribution. Surely, a practical realization of this system has an aperture hole connecting both lenses, but the conventional algorithm is not able to synthesize this finite aperture.

The next example demonstrates an anti-symmetry configuration for a couple of the Butler lenses. Its on-axis potential distribution

$$\Phi_-(z) = \begin{cases} \Phi_0 \left[3\left(\frac{z}{L}\right)^2 \left(1 - \frac{2z}{3L}\right) - 1\right], & 0 \le z \le L, \\ 3\Phi_0 \left(\frac{z}{L} - 1\right)^2 \left(1 - \frac{2}{3}\left(\frac{z}{L} - 1\right)\right), & L \le z \le 2L. \end{cases} \tag{26}$$

is shown with the curve $U2$ in Figure 3, but the off-axis potential distribution is described by the formula

$$\phi_-(r,z) = \begin{cases} \Phi_0 \left[3\left(\frac{z}{L}\right)^2 \left(1 - \frac{2z}{3L}\right) - 3r^2 \left(\frac{1}{2} - \frac{z}{L}\right) - 1\right], & 0 \le z \le L, \\ \Phi_0 \left[3\left(\frac{z}{L} - 1\right)^2 \left(1 - \frac{2}{3}\left(\frac{z}{L} - 1\right)\right) - 3r^2 \left(\frac{3}{2} - \frac{z}{L}\right)\right], & L \le z \le 2L. \end{cases} \tag{27}$$

This field is shown in the Figure 4b. It has a discontinuity for the second derivative of the axial potential $\Phi''(L-0) \ne \Phi''(L+0)$. The anti-symmetrical version of this system can not be synthesized in the classical formulation, because it is not clear how to take into account this discontinuity for $\Phi''(z)$. On the other hand our approach can easily overcome this obstacle by introducing the field sources - dipoles of unknown density ν, which can be determined by satisfying the Cauchy data.

These simplest configurations of the Butler lenses, presented above, have some disadvantages. One of them is that there are discontinuities for the second derivatives of the axial potential on the boundary of these lenses with equipotential or uniform-field region around the lens, which results in spatial beam aberrations. So we can consider the systems without this defect.

The first of these examples is a "matched" lens which creates a smooth transition from the uniform-field area to the equipotential space. The on-axis potential for this lens is represented by the cubic parabolas

$$\Phi_(z) = \begin{cases} 1 - \tilde{\alpha}z + \tilde{\beta}z^3, & 0 \le z \le \lambda, \\ \tilde{\gamma}(z-1)^3, & \lambda \le z \le 1. \end{cases} \tag{28}$$

Here λ is the position of the matching point, and the off-axis potential is described by the formula

$$\phi_-(r,z) = \begin{cases} 1 - \tilde{\alpha}z + \tilde{\beta}z^3 - \frac{3}{2}r^2\tilde{\beta}z, & 0 \le z \le \lambda, \\ \tilde{\gamma}(z-1)^3 - \frac{3}{2}r^2\tilde{\gamma}(z-1), & \lambda \le z \le 1. \end{cases} \tag{29}$$

The matching conditions for on-axis potential give us the relations

$$\tilde{\alpha} = \frac{3}{1+\lambda}, \quad \tilde{\beta} = \frac{1}{\lambda(1+\lambda)}, \quad \tilde{\gamma} = \frac{1}{\lambda^2 - 1}. \tag{30}$$

It is easy to verify the off-axis discontinuities $\delta E_z(r,z)$ at $z_1 = 0, z_2 = \lambda$ and $z_3 = 1$ for the accelerating fields. Normalizing these discontinuities to the maximum of the focusing field E_r, and evaluating its average value over the aperture dimension a, the defect of this field can be represented by the functional

$$I(\lambda) \equiv \frac{1}{a}\sum_i \int_0^a \left(r\frac{\delta E_{z,i}}{\max(E_r)} \right)^2 dr = a^4 f(\lambda), \tag{31}$$

where the summation is provided over all surfaces of discontinuity.

We name "optimal" the lens for which the functional $I(\lambda)$ reaches its minimum. By substituting the field distributions into the functional we obtain

$$\begin{aligned} I(\lambda) &= \frac{1}{a}\int_0^a \frac{r^4}{(3\tilde{\beta}\lambda)^2}\left(\frac{3}{2}\right)^2 \left[\tilde{\beta}^2 + (\tilde{\beta} - \tilde{\gamma})^2 + \tilde{\gamma}^2\right] dr = \\ & \frac{a^4}{20}\left[\frac{1}{\lambda^2} + \left(\frac{1}{\lambda} - \frac{1}{\lambda - 1}\right)^2 + \frac{1}{(\lambda-1)^2}\right], \end{aligned} \tag{32}$$

The extremum condition for $I(\lambda)$ leads us to a cubic equation

$$\lambda^3 + (\lambda - 1)^3 + \lambda^2 - (\lambda - 1)^2 = 0, \tag{33}$$

which has the only real root $\lambda_0 = 1/2$, and corresponds to a set of parameters

$$\tilde{\alpha}_0 = 2, \quad \tilde{\beta}_0 = \frac{4}{3}, \quad \tilde{\gamma}_0 = \frac{4}{3}, \quad I(\lambda_0) = \frac{6}{5}a^4. \tag{34}$$

An example of this lens is shown in the Fig. 5. There for the range $z = 0.45 \div 1.0$ one can see that the equipotential line $\phi = 0$ is a straight line $(z-1)^2 3/2r^2$, which separates the area of electrode-like surfaces from the lines cross the axis. Therefore there is a minimal value for the aperture $a_0 = \sqrt{2/3}(1 - \lambda_0)$, and electrode-like surfaces are absent for $a < a_0$. We call this the critical aperture . If the beam radius $r_0 < a_0$, then decreasing the transverse dimensions for the lens requires decreasing the critical value a_0, which is possible in non optimal choice for $\lambda > \lambda_0$. On the other hand, non linear beam aberrations are proportional to $(r_0/a_0)^4$, and more sensitive to

aperture value change than to increasing the function $f(\lambda)$. So we recommend making the optimal relation for the aperture

$$a = \begin{cases} r_0, & r_0 > a_0, \\ a_0, & r_0 \le a_0. \end{cases} \tag{35}$$

The second example includes an accelerating lens, which has equipotential regions with different potentials on both sides of the lens. It can be represented by an on-axis potential

$$\Phi_(z) = \begin{cases} \frac{1}{2}(1 - \tilde{\alpha}z + \tilde{\beta}z^3), & 0 \le z \le \lambda, \\ \frac{1}{2}\tilde{\gamma}(z-1)^3, & \lambda \le z \le 1. \end{cases} \tag{36}$$

$$\Phi(-z) = 1 - \Phi(z), \quad 0 \le z \le 1. \tag{37}$$

The matching conditions give us the optimal relation for the functional

$$I(\lambda) = \frac{a^4}{10}\left[\frac{1}{\lambda^2} + \frac{2}{\lambda(\lambda-1)^2}\right], \tag{38}$$

whose minimal value corresponds to the real root

$$\lambda_0 = \frac{1}{2}\left[\sqrt[3]{4 + \frac{2}{3}\sqrt{\frac{59}{3}}} + \sqrt[3]{4 - \frac{2}{3}\sqrt{\frac{59}{3}}}\right] \approx 0.4534. \tag{39}$$

The critical aperture value for this lens is $a_0 = \sqrt{2/3}(1 - \lambda_0) \approx 0.4463$.

Our third example is a single lens (Fig. 6), which is defined by an on-axis potential

$$\Phi(z) = \begin{cases} 1 - \tilde{\alpha}z + \tilde{\beta}z^3, & 0 \le z \le \lambda, \\ \frac{1}{2}\tilde{\gamma}(z-1)^3, & \lambda \le z \le 1. \end{cases} \tag{40}$$

$$\Phi(-z) = \Phi(z), \quad 0 \le z \le 1. \tag{41}$$

and the corresponding off-axis distribution

$$\phi(r,z) = \begin{cases} 1 - \tilde{\alpha}z + \tilde{\beta}z^3 - \frac{1}{2}r^2(3\tilde{\beta}z - \tilde{\alpha}), & 0 \le z \le \lambda, \\ \frac{1}{2}\tilde{\gamma}(z-1)^3 - \frac{3}{2}r^2(z-1)\tilde{\gamma}, & \lambda \le z \le 1. \end{cases} \tag{42}$$

$$\phi(r,-z) = \phi(r,z), \quad 0 \le z \le 1. \tag{43}$$

The matching conditions give us the optimal relation for the functional

$$I(\lambda) = \frac{a^4}{10}\left[\frac{3}{\lambda^2}(\lambda+1)^2 + \frac{2}{(\lambda-1)^2}\right], \tag{44}$$

whose minimal value corresponds to the cubic equation

$$\lambda^3 + \frac{3}{2}(\lambda^2 - 1)(\lambda - 1)^2 = 0, \tag{45}$$

which has a real root $\lambda_0 \approx 0.57095$. That gives the critical values

$$a_0 = \sqrt{\frac{2}{3}}(1 - \lambda_0) \approx 0.3503178, \quad I(\lambda_0) \approx 3.357632 a_0^4. \tag{46}$$

All examined lenses are different configurations of basic lenses. You can get an electron optic system of arbitrary configuration using this basic set, which forms the cylindrical beams with defined energy features.

5 Results of numerical simulations

We have used the code "Synthesis-2" to model the following examples. In numerical simulation of the Butler lenses with total length $2L$ shown in the Fig. 4 a, the total number of nodal values for sources was $N = 48$ and $L = 1$. The accuracy of the solution reproduction in the area $z \in [0, 2] \times r \in [0, 1]$ was $\delta\phi/\phi \approx 5 \cdot 10^{-4}$ with the weight coefficient $w^2 = 2 \cdot 10^{-3}$ for the "skeleton" surface, which was chosen to be a straight line $z = 1$. The accuracy was evaluated at the nodes of rectangular mesh 11×12 covering the simulated domain. However that problem has no practical interest because of the absence of the hole between lenses, and so we examined a modified problem (Fig. 7). Here the Cauchy data have been defined on the segment $0.5 \leq z \leq 1.5$, and the "skeleton" surface ended on the distance $r = 0.1$ from the axis. The external electrodes on the boundary of the rectangular domain have Dirichlet conditions (24). The Figure 7 represents a map of equipotential lines for two different values of the weight coefficients. The relative error for the extrapolated potentials was $\delta\phi/\phi \approx 5 \cdot 10^{-3}$. These two simulations a) and b) have been done to determine the band of tolerances for the geometry of the electrodes. This band can be obtained by superposition of two maps of equipotentials.

A less evident map of equipotential lines corresponds to the anti-symmetrical configuration of the Butler lenses shown in the Fig. 8. Here introducing of the "skeleton" surface with dipole sources creates the pairs of electrode-like surfaces with positive and negative potentials.

The Figs. 9 and 10 show examples of the analytical continuation problem, where a synthesized fragment must be embedded into some external a priori defined field. In our case the external field is expanded through the upper boundary, where we defined a uniform Neumann condition $\partial\phi/\partial\vec{n} = 0$, and linear Dirichlet condition. This potential for the symmetric configuration is

$$\phi(1, z) = \begin{cases} 4z - 1.5, & 0 \leq z \leq 1, \\ -4(z-1) + 2.5, & 1 < z \leq 2, \end{cases} \tag{47}$$

and for anti-symmetric one is

$$\phi(1, z) = \begin{cases} 4z - 2.5, & 0 \leq z \leq 1, \\ 4(z-1) - 1.5, & 1 < z \leq 2. \end{cases} \tag{48}$$

In the case the upper boundary plays the role of the axis with the Cauchy data.

The following Figs. 11, 12 and 13 show the results of numerical synthesis for matching, accelerating and single lenses with different sizes of the aperture holes. The stability of numerical solution decreases when the aperture dimension a is less then its critical value a_0. In that case the smoothness of equipotential lines is decreased.

Solving self-consistent problem for a cylindrical beam does not introduce the new moments to the synthesis procedure. However in this case the problem is non linear, and we use an iterative procedure to take into account the space charge effects. We note that structure of the on-axis field for a beam with space charge given by a formula

$$\rho(r, z) = h(z) + r^2 g(z), \quad r \leq R_0, \tag{49}$$

which is a cubic polynomial of z, leads us to the linear focusing components of the field $E_r(r, z) \sim r$. Here R_0 is a radius of a beam, $h(z)$ and $g(z)$ are some smooth functions. Thus, using (49), we can compensate the geometric aberration due the space charge effects by satisfying the Cauchy data for the ideal parallel beam. The results of numerical simulations are shown in the Fig. 14. In our case the initial energy for the particles was eqial to 4 KeV, and perveance $P = 0.55\mu A/V^{3/2}$. The trajectories of the beam are practically parallel.

The next Fig. 15 gives an example of numerical synthesis of focusing electrodes for a Pierce gun and for post-accelerating section for this gun. Here the cathode electrode was fixed in shape with potential $\phi = 0$, the upper boundary had a linear distribution of potential to prevent vacuum breakdown, but the shapes of focusing electrodes were synthesized.

The last example presents the results of numerical synthesis for an insulator of an accelerating tube. The outer boundary for that insulator is a ceramic cylinder (c), internal cylinders (i) are accelerating electrodes. The goal is to synthesize the shape for tops of electrodes, which overlap the area of direct line of sight from the beam to ceramic and provide minimal values for the field strength, because one of the reason for the breakdown in high vacuum is induced by the particles crossing the gap and acummulating on ceramics. Figure 16 shows the results of simulations with different values for the weight coefficients.

6 Conclusions

Our publications [30],[34] are devoted to the detailed description of the algorithm for solving the synthesis problem and to models of electron lenses with minimal aberrations forming the round beams. One of the advantages of our approach is that it can evaluate the tolerance to geometry variations for the previously defined optical quality requirements.

We also pay attention to the problem of analytical continuation of the solution through the boundary of arbitrary shape. To solve this problem, some assemblies and subsystems of the device are considered fixed, and the problem is to extrapolate the the fields of these parts to some embedded fragment of the device in a smooth way.

We will also present the results of numerical simulations for the test and practical problems provided using our code "Synthesis-2", which is devoted to solving 2D problems of electron optics similarly to the earlier code "Poisson-2" [31]. Both are included in the "TOPAZ" CAD system [32]. The ideas of the practical approach to 2D synthesis problems can be applied to 3D problems without any restrictions, for example, with the code "Poisson-3" [33].

7 Acknowledgments

Our special thanks go to V. Dolgashev for stimulating discussions, to G.B. Bowden and G. Schussmann for assistance with preparation of the manuscript.

References

[1] J.R. Pierce. Theory and Design of Electron Beam, Van Nostrand, 1949, 1954.

[2] B. Meltzer. Proc. Phys. Soc., 62, 355 (1949) 431.

[3] P.J. Lomax, J. of Electronics, 3, 4(1957)367.

[4] P.T. Kirstein, Proc. IRE, 46, 10 (1958)1716.

[5] P.T. Kirstein, J. Appl. Phys., 29, 12 (1958)1758.

[6] K.J. Harker, J. Appl. Phys., 31,12(1958)2865.

[7] von W. Tretner, Optik, B. 16, 3(1959)155.

[8] M. Szilagyi. Electron and Ion Optics, Plenum Press, 1988.

[9] V.T. Ovcharov, Dokl. Akad. Nauk SSSR, 107,1(1956)47.

[10] V.T. Ovcharov,Radio. Eng. Enectron. Phys. (USSR), 6(1957)696.

[11] V.T. Ovcharov,B.T. Kormilitsyn, Radio. Eng. Enectron. Phys. (USSR), 7(1960)1112.

[12] V.T. Ovcharov, . Eng. Enectron. Phys. (USSR), 8(1962)1367.

[13] V.T. Ovcharov, Radio. Eng. Enectron. Phys. (USSR), 8(1970)1651.

[14] V.T. Ovcharov, V.V. Penzyakov, Radio. Eng. Enectron. Phys. (USSR), 9(1970)1897.

[15] V.N. Danilov, V.A. Syrovoy, Prikladnaya Matematika i Mechanika, 35, 4(1971)656.

[16] V.N. Danilov, V.A. Syrovoy, Radiofizika, 20, 11(1977)1727.

[17] V.N. Danilov, S.S. Drozdov, Y.V.Lavrent'ev et al., Elektronnaya Technika, ser. I, 2(1976)53.

[18] V.A. Syrovoy, Prikladnaya Matematika i Mechanika, 34,1(1971)4.

[19] V.A. Syrovoy. In: New methods of design of electron-optic systems. Moscow, Nauka, (1983) 55.

[20] V.A. Syrovoy, . Eng. Enectron. Phys. (USSR), 4(1985)793.

[21] L.P. Shanturin, Radio. Eng. Enectron. Phys. (USSR) , 3(1980)612.

[22] M.A. Monastyrsky, Zh. Tekh. Fiz., 56,4(1986)625.

[23] G.G. Gurbanov, P.P. Kasiankov, I.N. Taganov, Radio. Eng. Enectron. Phys. (USSR) , 4(1967)659.

[24] P.N. Vabischevich, Zh. Vychislitel'noy Matematiki i Matematicheskoy Fiziki, 2(1981)509.

[25] A.I. Volodin, V.A. Danilov, V.V. Slaviansky. In: Algorithms and Methods of design of Electron-Optic Systems, Novosibirsk, (1983)108.

[26] S.I. Molokovsky, A.D. Sushkov. High-current Electron and Ion Beams, Leningrad, Energiya, 1972.

[27] P.I. Akimov, V.A.Syrovoy, A.B.Tskhai, Radio. Eng. Enectron. Phys. (USSR) , 7(1985) 1409.

[28] A.V. Vashkovski, E.A. Soluyaniva, V.A. Syrovoy, S.E. Tsimring, Radio. Eng. Enectron. Phys. (USSR), 4(1986) 783.

[29] L.A. Neganova, V.A. Syrovoy, V.N. Tskhai, Radio. Eng. Enectron. Phys. (USSR) , 10(1990) 2146.

[30] V.Breznev, N.Dikansky, V. Ivanov, Practical Approach to Synthesis Problems of Electron Optic Systems, Preprint 103(1986), BINP RAS.

[31] V. Astrelin, V. Ivanov, Avtometria, 3(1980)92.

[32] V. Ivanov. CAD methods in physical electronics. In 2 parts. Novosibirsk, Inst. Math. RAS, 1986.

[33] V. Ivanov. Proc. VIII Conf. on Comput. Meth. in Electron Optics, Jan. 1985, Leningrad, Russia, (1985)98.

[34] V. Brezhnev,V. Ivanov, Proc. Institute of Mathematics SB AS USSR, 15(1989)187.

[35] J.H. Alberg, E.N. Nilson, J.L. Walsh, The Theory of Splines and Their Applications, Academic Press, 1967.

[36] J.W. Butler, Kyoto, 1(1966)191.

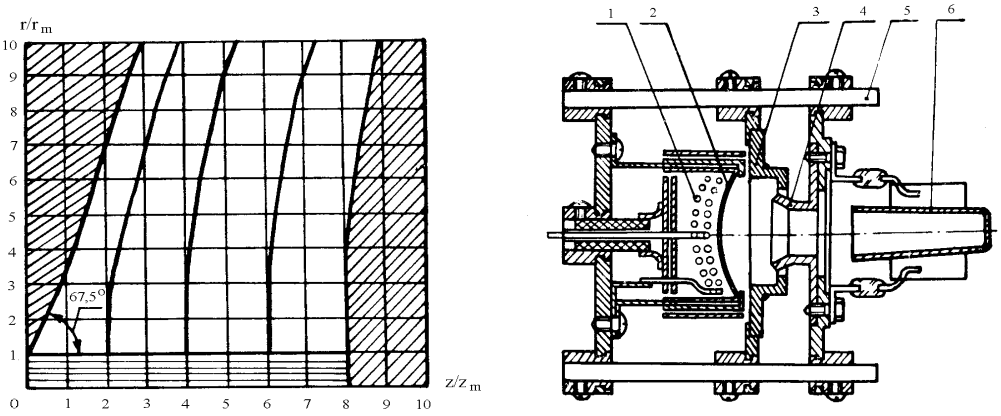

Figure 1: Analytical solution for the Pierce gun and the real Pierce gun. Courtesy of [26], p.12 and 161. 1 - heater; 2 - cathode; 3 - grid; 4 - anode; 5 - ceramic insulator; 6 - collector

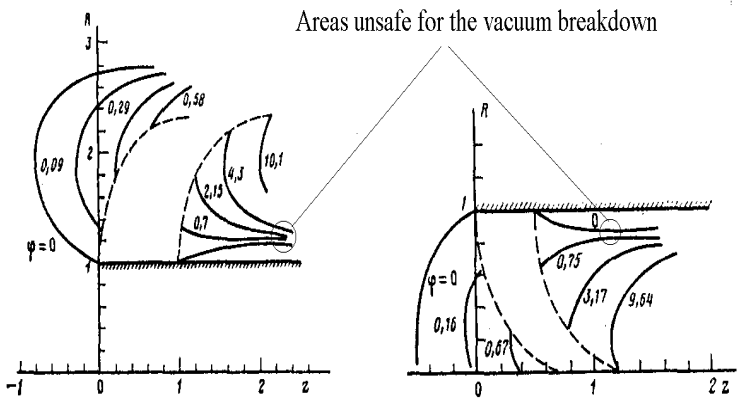

Figure 2: The results of numerical synthesis in the classical formulation. Courtesy of [28]. Dashed lines show the nominal beam boundary.

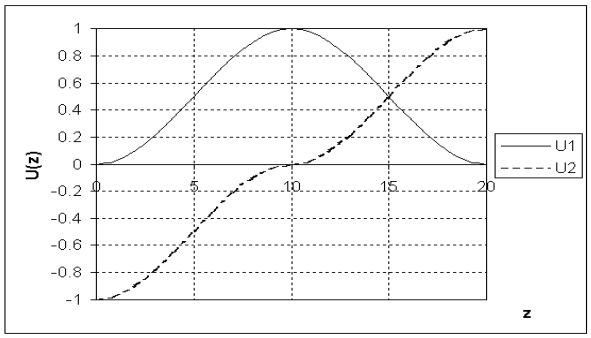

Figure 3: On-axis potential for a couple of Butler lenses. U1 - symmetrical case; U2 - anti-symmetrical case.

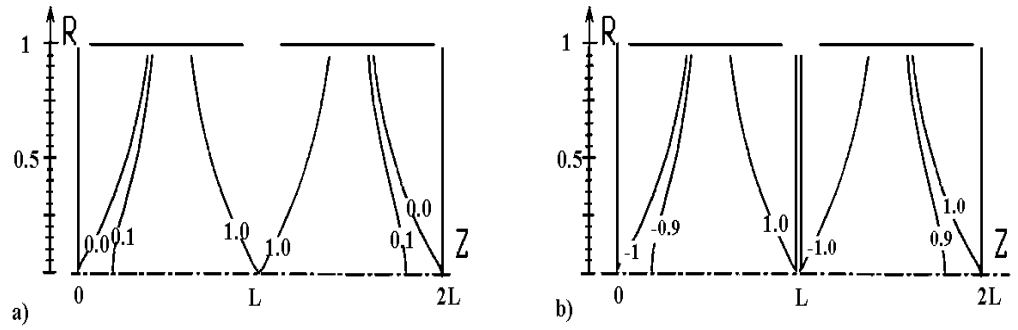

Figure 4: Off-axis potentials for a couple of Butler lenses, a) symmetrical configuration; b) anti-symmetrical case.

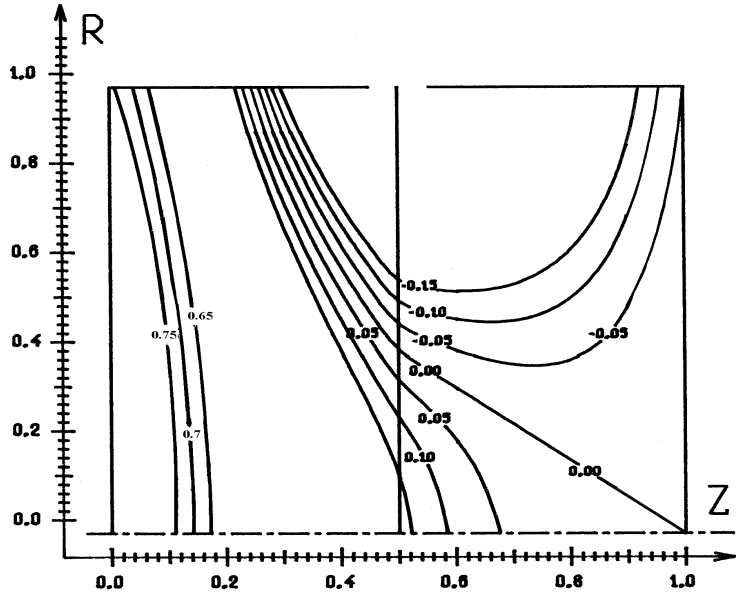

Figure 5: The ideal matching lens.

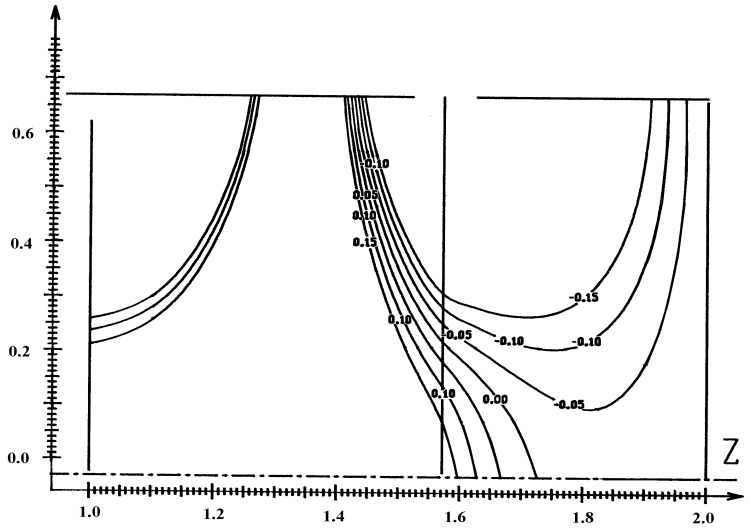

Figure 6: The ideal single lens.

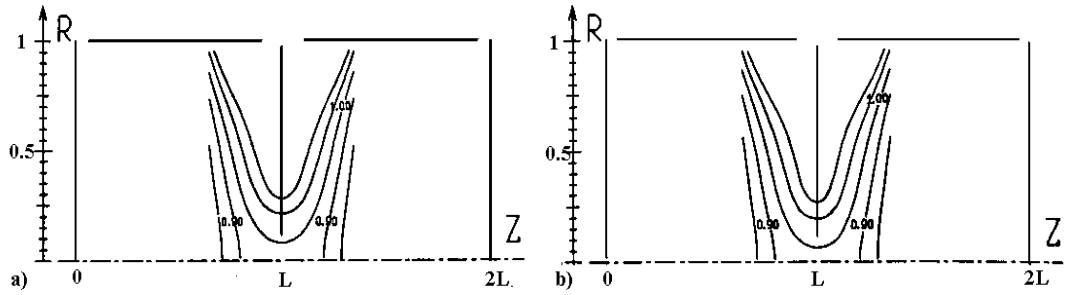

Figure 7: The results of numerical synthesis for a couple of Butler lenses. Symmetrical case, a) $w = 0.09$; b) $w = 0.2$.

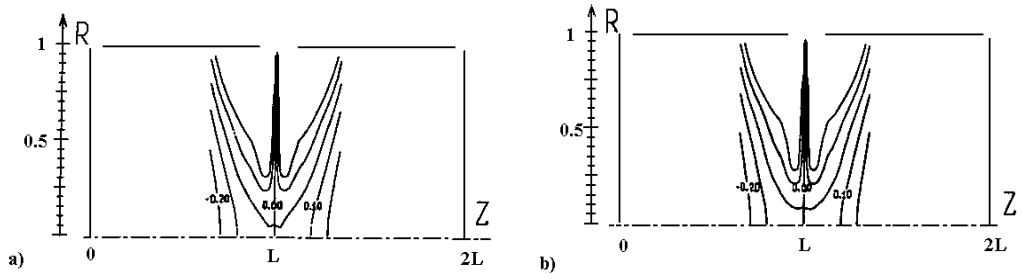

Figure 8: The results of numerical synthesis for a couple of Butler lenses. Anti-symmetry case, a) $w = 0.09$; b) $w = 0.2$.

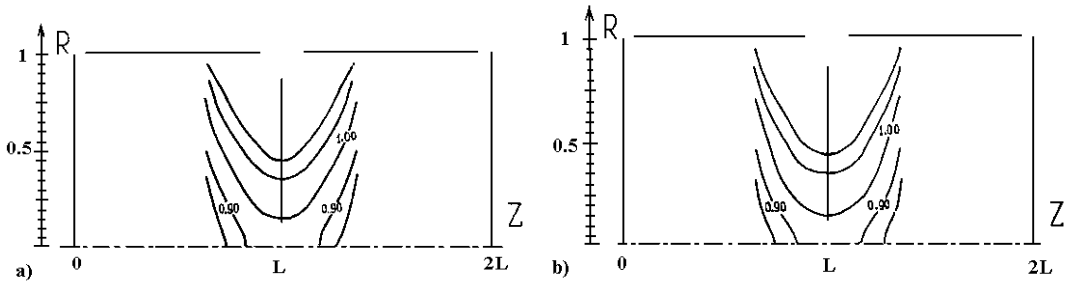

Figure 9: Analytical continuation of the field. Symmetric case, a) $w = 0.2$; b) $w = 0.22$.

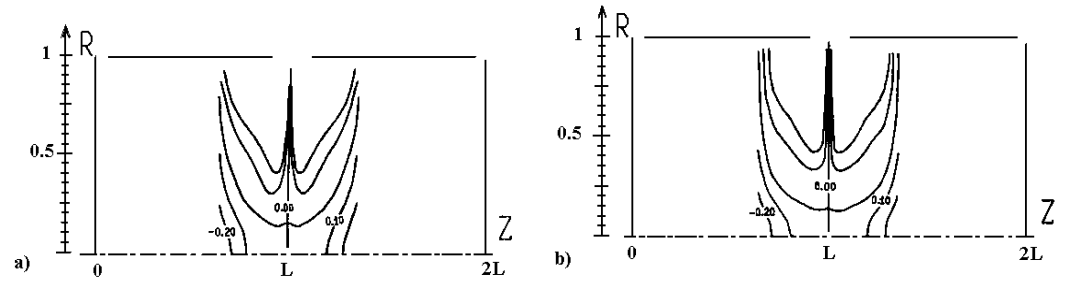

Figure 10: Analytical continuation of the field. Anti-symmetric case, a) $w = 0.09$; b) $w = 0.2$.

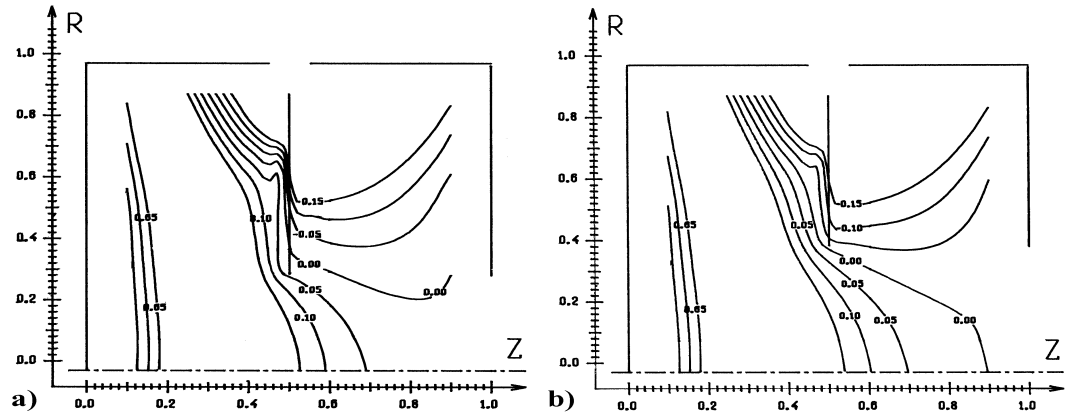

Figure 11: The results of numerical synthesis for a matching lens, a) aperture a=0.3; b) aperture a=0.4.

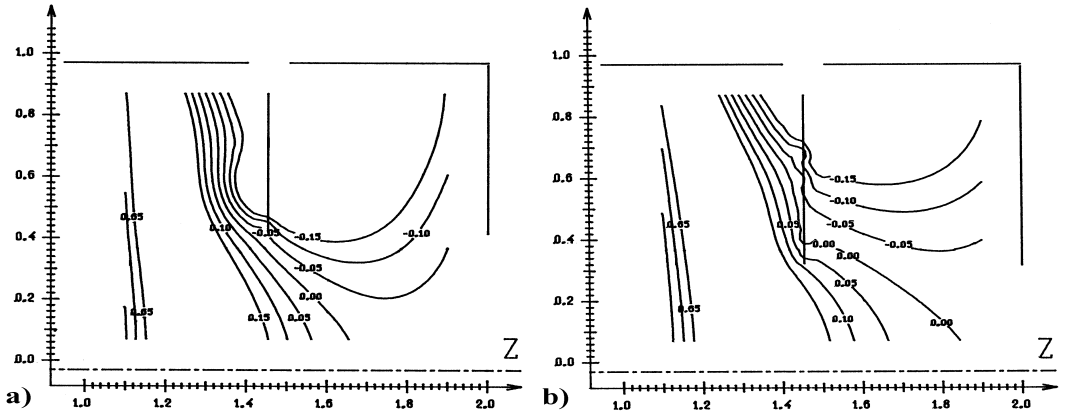

Figure 12: The results of numerical synthesis for an accelerating lens, a) aperture a=0.3; b) aperture a=0.4.

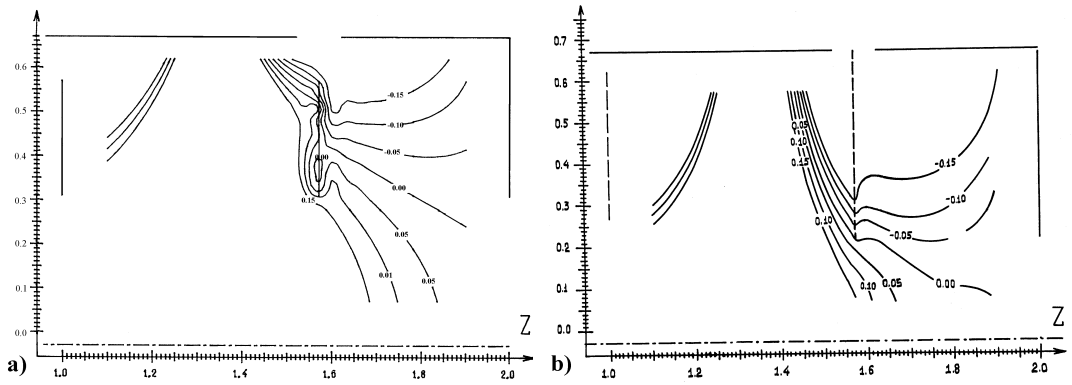

Figure 13: The results of numerical synthesis for a single lens, a) aperture a=0.3; b) aperture a=0.43.

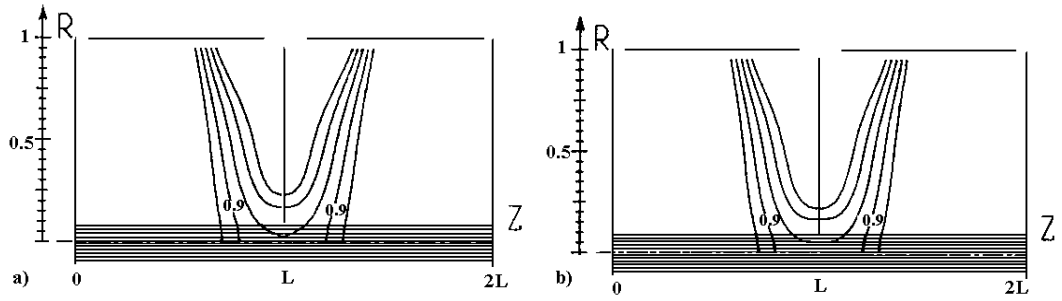

Figure 14: The results of numerical synthesis for the Butler lens with cylindrical beam , a) $w = 0.09$; b) $w = 0.2$. Equipotential lines and trajectories are shown.

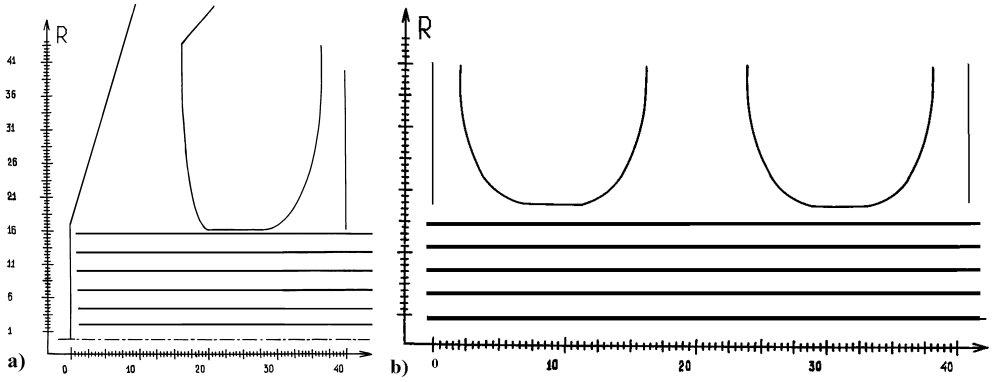

Figure 15: The results of numerical synthesis for the Pierce gun a) and post-accelerating section b). Equipotential lines and trajectories are shown.

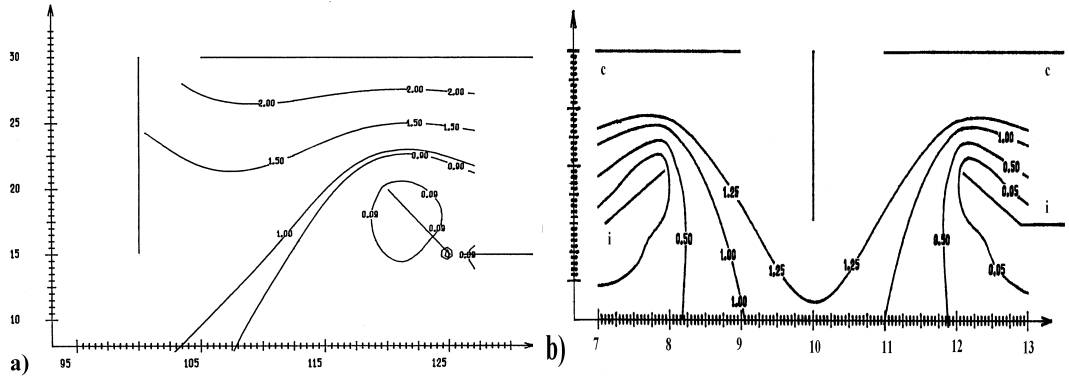

Figure 16: Numerical synthesis for the insulator, a) $w = 0.09$; b) $w = 0.2$.